Acta Mechanica Slovaca **26 (3): 32- 41,** September **2022**
https://doi.org/10.21496/ams.2023.002

Acta Mechanica Slovaca
ISSN 1335-2393
www.actamechanica.sk

Numerical Simulation of Heat Transfer Behaviors in Conical Pin Fins Heat Sinks

Sayah Souida[1], Djamel Sahel[1,2]*, Houari Ameur[3], Aissa Yousfi[1]

[1] Technical Sciences Department, Amar Telidji University of Lagouat, Laghouat,03000,Algera
[2] Gas Fuels and environment laboratory (LCGE), USTO-MB, Oran,31000, Algeria
[3] Department of Technology, University Centre of Naama - Ahmed Salhi, P.O. Box 66, Naama, 45000, Algeria

Abstract: The present study is a numerical investigation of the effect of the shape of pin fins on the overall performances of heat sinks. Conical shaped pin fins with varying conical size ratio (*Hcp/d*) are considered. Five geometrical cases are explored, namely *Hcp/d* = 0.167, 0.333, 0.500, 0.667 and 0.833. The distribution and values of temperature, Nusselt number, thermal resistance, pressure drop, as well as the hydrothermal performance factor are determined for various Reynolds numbers (up to 8,000). In addition, the performances of conical shaped fins are compared to those of the cylindrical fins. The obtained results revealed a decrease in the thermal resistance with increasing *Re* and *Hcp/d* ratio. At *Re* = 8000 and when changing (*Hcp/d*) from 0.167 to 0.833, the thermal resistance is decreased from 192.30% to 83.52% compared to the cylindrical pin fins. However, the increased (*Hcp/d*) ratio yields an increase in the pressure drop. At *Re* = 8000, the values of pressure drop for the conical fins are lower than those of the cylindrical fins by 343.32%, 275.92%, 205.79%, 144.86% and 100.38% for *Hcp/d* = 0.167, 0.333, 0.500, 0.667 and 0.833, respectively. The values of the hydrothermal performance factor (η) for the conical fins are greater than those of the cylindrical fins. Also, an increase in (η) values is observed with decreasing *Hcp/d* ratio. The highest (η) value of 1.51 is reached with the case *Hcp/d* = 0.167 at *Re* = 8,000.

Keywords: Heat sinks; Conical shaped fins; cylindrical fins; hydrothermal performances

1. Introduction

Concerning the developments in the electronics applications in the last years, electronic devices are becoming smaller than the classical systems, and this miniaturization leads to very small designs. This development has created another challenge; it consists of the increase in heat which can damage electronic tools. Against this background, experts have become faced with the problem of cooling methods in a limited space. Phase change cooling [1,2], nanofluids [3–6], hybrid nanofluids [7–10], porous medium [11,12] are important methods for cooling of the electronic devices, but in view of their production costs and technical complexity, these methods still remain relatively inapplicable to the electronic tools design [13]. However, the cooling by using air impingement presents a reliable solution to the heat dissipation in heat sinks (*HSs*) [14]. For this solution, several techniques were largely used in the HSs design, such as the perforation space, vortex generators (*VGs*) and the shape of pin fins innovation.

The perforation space through heat sink presents a successful method to enhance the heat dissipation rates and fluid flow structures [15]. Where, the perforation space helps to reduce the lowers heat transfer areas (*LHTA*) behind of the pin fins by better air flow swirling. In the other hand, this method can reduces the pressure drop a long of heat sink by reducing of blockage flow phenomena around of the pin fins [16–18]. Chin et al [19] numerically and experimentally investigated the effects of size and number of

* **Corresponding author:** Djamel Sahel, ***E-mail address:*** *d.sahel@lagh-univ.dz*

holes in pin fins heat sinks (*PFHS*). They reported that the heat transfer coefficient of the perforated *PFHaS* was augmented by 45 % compared with solid pin fins. In addition, the pressure drop was also reduced by 18% for the same comparison. Kore *et al* [20] confirmed that the perforation space through the pins fins can increases the heat transfer rates, where for 5 holes, Nusselt number was increased by 23% compared with the conventional pin fins. In general, perforation technique directly influence on the heat transfer and pressure drop characteristics in heat sinks [21,22].

The location of vortex generators (*VGs*) or baffles inside *PFHS* present another solution to enhance heat dissipation rates of heat sinks. For all the thermal systems, *VGs* helps de destruct thermal and hydrodynamic boundary layers, with are improve heat transfer execution [23–28]. Karami *et al* [29] numerically simulated by using ANSYS Fluent the effects of baffles on fluid flow and heat transfer characteristics of a micro channel heat sink. They used single segmental baffle, double segmental baffle, and triple segmental baffle for different overlaps namely 60%, 40%, 20% and 0%. They used micro pin fins heat sink without baffle as a reference case of comparison. They concluded that heat transfer coefficient of 20% overlaps double segmental baffle and $Re = 250$ was augmented by 47, 37% compared with the reference case. Khosvaght-Aliabadi *et al* [30] optimized the thermal and hydraulic performances of miniature heat sink (*MHS*) by using nanofluid-cooled zigzag. For this purpose, they experimentally examined six (06) pin fins interruptions. They reported that zigzag configuration of pin fins heat sink has a considerable effect on the *MHSs* design. Khan *et al* [31] tested the effects of different shapes as *VGs* on the heat transfer performance of a micro pin fins heat sink. Rectangular, semi-circular, rectangular/triangular, rectangular/semi-circular, and triangular/circular are the six configurations were used to examine the performance of the micro pin fins heat sink. They reported that the triangular ribs were significantly reducing the thermal resistance of the micro pin fins heat sink. On the other hand, this configuration was also generating a largest pressure drop.

The shape of pin fins was also a successful strategy for heat sinks design. Several authors reported that the pin fins form plays an important role to improves thermal dissipation in heat sinks [32–34]. Leong *et al* [35] used paraffin wax and 1-hexadecanol based heat sinks to reduce the operating temperature of electronic device. They reported that combination between phase change materials (*PCMs*) and paraffin wax and 1-hexadecanol based heat sinks can enhance heat dissipation in heat sinks. Also, they concluded that heat sinks filled with paraffin wax performed better than heat sinks filled 1-hexadecanol. Shi *et al* [36] analyzed some geometric parameters on the performance of a micro-channel heat sinks. They proposed a design include the secondary channel width ratio to micro-channel width (a), the half pitch ratio of secondary channel to micro-channel width (β) and the tangent value of secondary channel angle (γ). Compared with smooth channel, the thermal resistance (R_{th}) and the pumping power (P_p) of the micro-channel with secondary flow channel can be minimized by 28.7% and 22.9%, respectively. In an experimental study, Sathe and Sanap [37] compared between plain rectangular fins and slitted rectangular fins. They found that the heat transfer coefficient augmented by 58% for silted rectangular fins, compared with plain rectangular fins. In general, it's exist several shapes which can improve the heat dissipation in heat sinks such as oblique fins [38], honeycomb heat sink [39], semi-circular/semi-elliptic [40].

Considering all that has been discussed already, it has been concluded that the shape of pin fins can respond to the worry of experts for the heat sinks manufacture. With the help of this technique, the thermal performance may be increased; also, the occupancy volume and size of heat sinks and the pressure loss during their operation may be reduced. For this purpose, the effect of conical pins fins on the air fluid flow and heat dissipation behaviors of heat sinks are tested in this paper. The investigations are performed for conical size ratio (*Hcp/d*) varying from 0.167 to 0.833. The temperature, Nusselt number, pressure difference, thermal resistance and the hydrothermal performance factor are the parameters used for the evaluation tasks, and promising results were found.

2. Model description

The PFHSs consisting of a base plate and staggered conical fins placed on the base plate were mounted in a channel as depicted in Fig.1. The dimensions of the channel (L_1, L_2, and H) and the base plate (L_b, W, and e_b) were summarized in table 1. The fins and the base plate were made of

A8350P type aluminum. The cylindrical pin fins used by Chin *et al* [19] were used to validate the present model. After the validation task, a parametric study was focused to examine the effects of conical pin fins size under fully turbulent flow conditions.

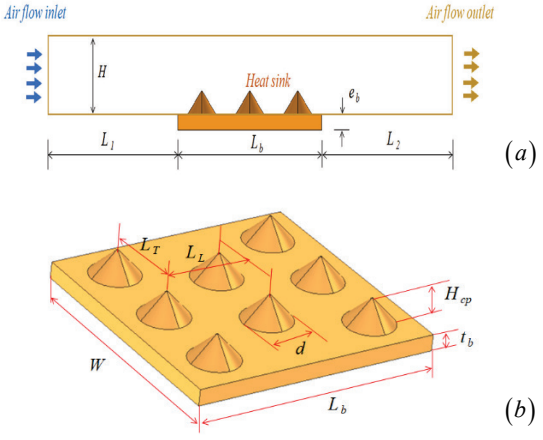

Figure 1: Configurations of, a) channel and, b) pin fins heat sinks.

Table 1: Dimensions of channel heat sinks and base plate, in (mm).

L_1	L_2	H	W	L_b	e_b	d
70	70	8	30	30	2	6

3. Numerical model

The fluid flow and heat transfer behaviors through *PFHSs* were numerically analyzed by using COMSOL v.5.4 software. From this software, no isothermal flow interface was used to investigate the fluid flow and conjugate heat transfer. The conduction heat transfer was set through the solid-Aluminum, where the heat transfer by convection implanted by the contact the wall solid-Aluminum and the air flow.

The turbulent air flow enters at 300 K, for Reynolds number (*Re*) varying from 3000 to 8000. The governing equations for steady-state and incompressible fluid flow are determined as follows;

Continuity equation

$$\frac{\partial u_i}{\partial x_i} = 0 \tag{1}$$

Momentum Equation

$$\frac{\partial (u_i u_j)}{\partial x_j} = \frac{\partial \overline{p}}{\partial x_i} + \nu \nabla^2 u_i + \frac{\partial}{\partial x_j}\left(\overline{u_i' u_j'}\right) \tag{2}$$

Energy Equation

$$\frac{\partial (u_j T)}{\partial x_j} = \alpha \nabla^2 T + \frac{\partial}{\partial x_j}\left(\overline{u_i' \theta}\right) \tag{3}$$

Heat Conduction Equation

$$\nabla\left(\lambda_s \nabla T_s\right) = 0 \tag{4}$$

For closing of the equations system, the RANS-based k-ε turbulence model is used in this paper as a robust model which is largely utilized for some industrial applications [15,19].More details of this turbulence model can be found in the COMSOL v.5.4 CFD User's guide [41].

For performance evaluation task of heat sinks, the Nusselt number (*Nu*), the thermal resistance (R_{th}), the pressure drops (Δp), and the thermo-hydraulic performance factor (η) are the fundamental parameter used in this paper. These parameters are calculated and summarized respectively as follow.

$$Nu = \frac{q'' D_h}{\lambda_{air}\left[T_w - (T_{in} + T_{out})/2\right]} \tag{5}$$

$$R_{th} = (T_w - T_{in}) / q'' \tag{6}$$

$$\Delta p = p_{in} - p_{out} \tag{7}$$

$$\eta = \frac{\left(Nu / Nu_{CPFS}\right)}{\left(\Delta p / \Delta p_{CPFS}\right)} \tag{8}$$

For the flow regime determination, the Reynolds number (*Re*) was used as follow:

$$\mathrm{Re} = \frac{U_{in} D_h}{\nu} \tag{9}$$

Where, D_h is the hydraulic diameter and determined as:

$$D_h = \frac{4 \times A_c}{P} \tag{10}$$

Where, P and A_c are the perimeter and cross section of channel, respectively.

The mesh independency, it structures and number play important role in the reliability of the results of numerical model. For this reason, the Nusselt number results acquired by means of generated tetrahedral meshes type having various numbers of elements were compared with each other. A grid sensibility test was done for *CPFHSs* at *Re*=8000. In this context, a series of grids containing 511,298, 762,434, 988,353, 1,113,774 and 1,344,617 were realized. Compared with 988,353 elements case, the results found that the Nusselt number variation of the grids of greater elements

(1,113,774 and 1,344,617) is less than 1.3 %. As a consequence, the grid 988,353 elements were utilized in the definitive *CPFHSs* investigations. The same strategy of meshing test was followed for other configurations as well.

4. Results and discussion

4.1. Validation of results

In order to validate the reliability of the present numerical model, we based on the experimental data of Chin et al [19]. The comparison was based on the results of Nusselt number (*Nu*) and pressure drop (*Δp*). As shown in Fig. 2, the comparison between the results of the present work and reference [19] indicate a satisfactory agreement.

4.2. Thermal and hydrodynamic aspects

As known in literature, fluid flow structure directly affects the thermal field. In particular, convective heat transfers mainly related by the fluid flow characteristics. For this reason, we based on the wall velocity (Fig.3) and wall temperature (Fig.4) contours to explain the fluid flow structure and thermal field respectively. From Fig.3, the air flows thorough the conical pin fins and base plate and creates two primordial zones; the first is the reattachment zone at height velocity which appear in red color in the sides of the pin fins. The second is appear in the blue color with presents the recirculation fluid flow zone upstream and downstream of pin fins at feeble values of velocity.

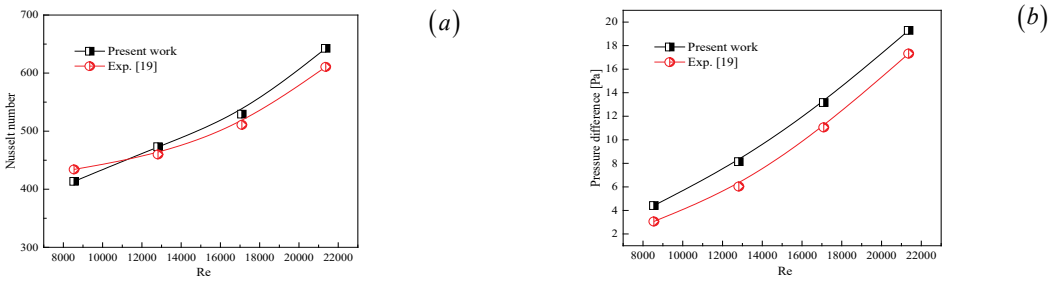

Figure 2: Validation of result, a) Nusselt number and b) Pressure difference.

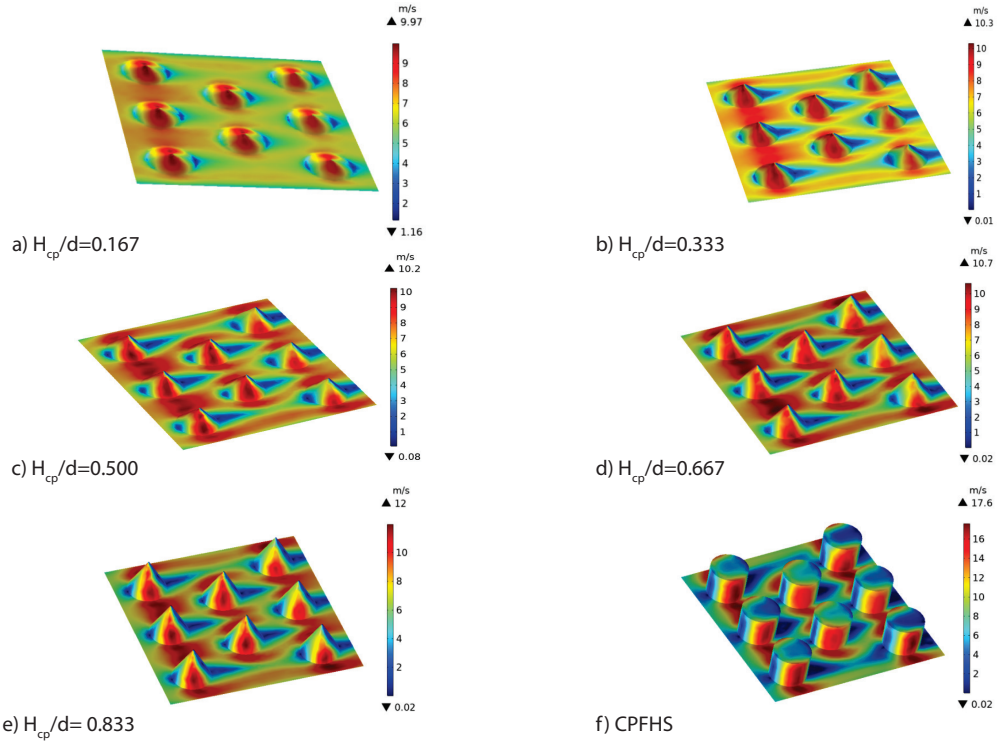

Figure 3: Contours of wall velocity, Re=8000.

The last phenomenon's directly influence the thermal field as shown in Fig.4. Where, the first zone at height velocity helps to reduce the lower heat transfer areas (*LHTAs*) as appeared in yellow color. The recirculation fluid flow zones create the *LHTAs* after and before of the pin fins which are reduce the heat transfer coefficients in these zones. As observed from Figs. 3 and 4, the augmentation of *Hcp/d* ratio tend to an undesirable formation of *LHTAs*.

4.3. Heat transfer coefficient

Fig. 5 depicts the variation of Nusselt number (*Nu*) versus Reynolds number (*Re*). For all cases, Nusselt number (*Nu*) raises with rising Reynolds number (*Re*) for *Co-PFHSs* having various *Hcp/d* and their comparison with that reference case (*CPFHS*). It is clear from the figure that Nu raises with rising *Re* and *Hcp/d* ratio. This is for the reason that the rising *Re* and *Hcp/d* ratio means that rising flow inlet velocity and global heat transfer surface. The results show that Nusselt number is decreased by 194.14%, 169.72%, 138.73%, 112.12% and 85.12% for Hcp/d=0.167, 0.333, 0.500, 0.667 and 0.833 compared to the reference case at *Re* = 8000, respectively.

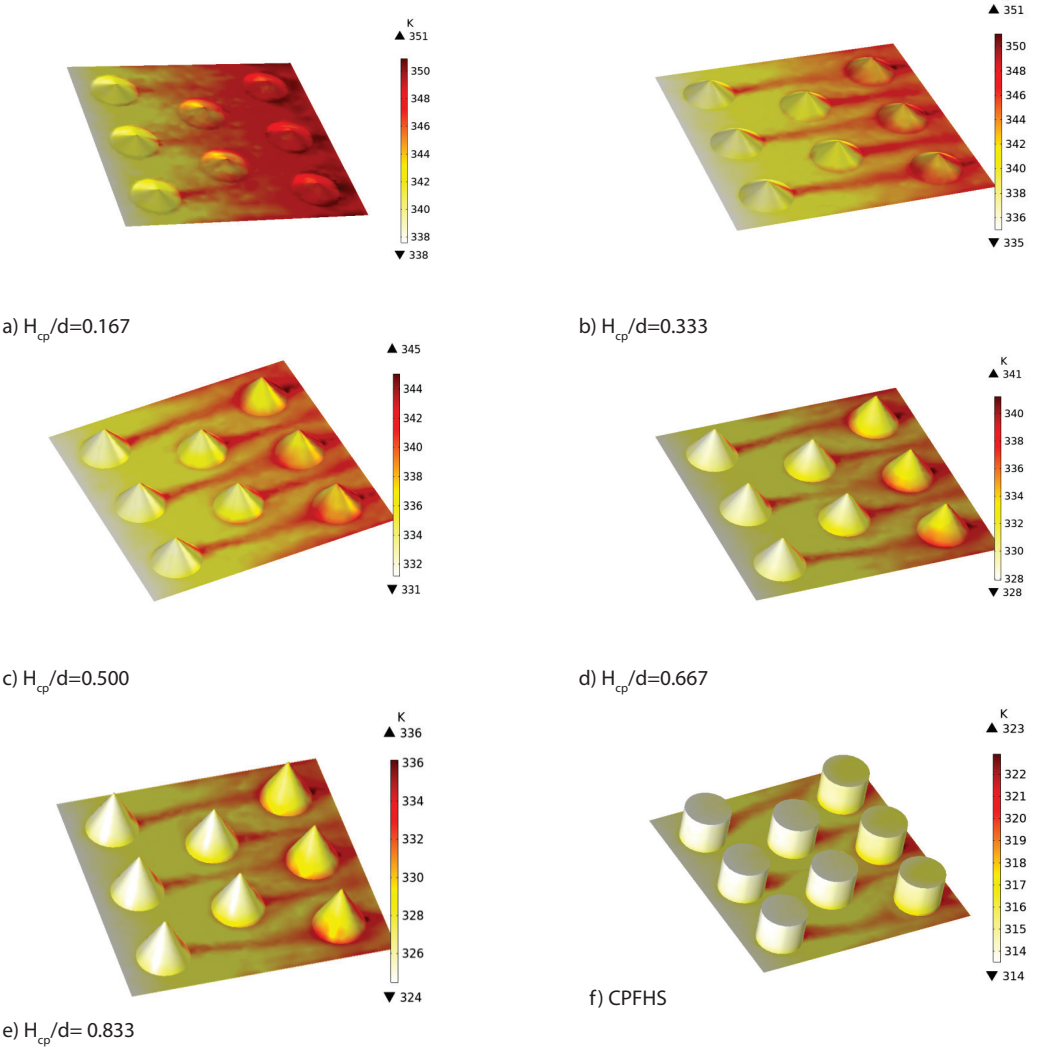

a) H_{cp}/d=0.167

b) H_{cp}/d=0.333

c) H_{cp}/d=0.500

d) H_{cp}/d=0.667

e) H_{cp}/d= 0.833

f) CPFHS

Figure 4: Contours of wall temperature, *Re*=8000.

4.4. Pressure drops

Fig. 6 depicts the variation of *Δp* versus *Re* for *Co-PFHS* having various *Hcp/d* ratios and their comparison with the reference case (*CPFHS*). It is easy to see from the figure that the decreased Hcp/d of *Co-PFHS* leads to a very significant decrease in the pressure drop compared with *CPFHS*. Fortunately, the results show that *Δp* is decreased by 343.32%, 275.92%, 205.79%, 144.86% and 100.38% for Hcp/d=0.167, 0.333, 0.500, 0.667 and 0.833 compared to the reference case (*CPFHS*) at *Re* = 8000, respectively. So, the *CPFHS* is not advised to design heat sinks due to the dramatically increase in the pressure drop compared with the present configurations (*Co-PFHS*). These increases of pressure drop are due to the flow blockage phenomena upstream of pin fins (Fig. 7).

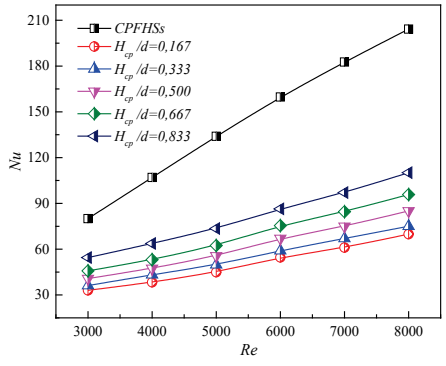

Figure 5: Nusselt number (*Nu*) vs. Reynolds number (*Re*).

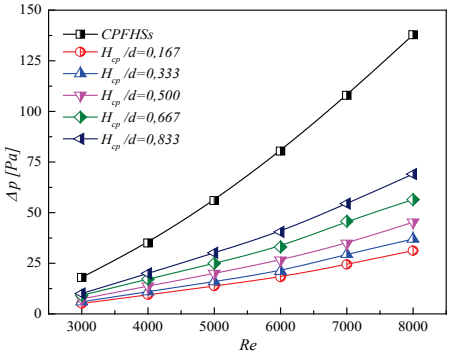

Figure 6: Pressure difference (*Δp*) vs. Reynolds number (*Re*).

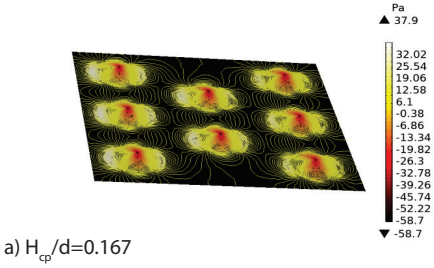

a) $H_{cp}/d=0.167$

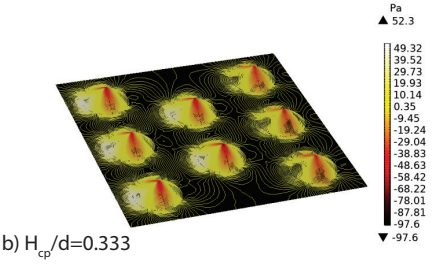

b) $H_{cp}/d=0.333$

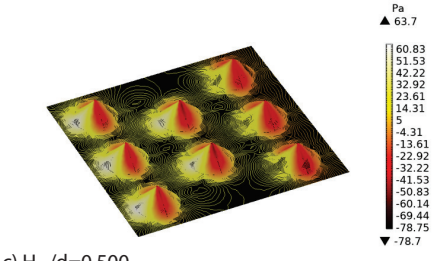

c) $H_{cp}/d=0.500$

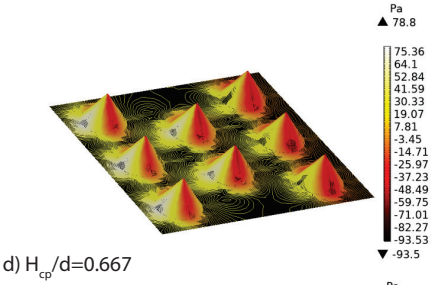

d) $H_{cp}/d=0.667$

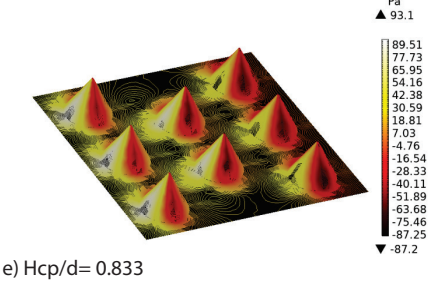

e) Hcp/d= 0.833

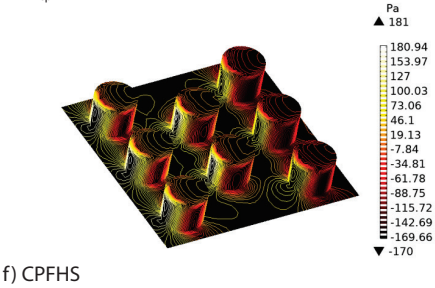

f) CPFHS

Figure 7: Static pressure distribution, *Re*=8000.

4.5. Thermal resistance

Fig. 8 presents the variation of R_{th} according to *Re* for *Co-PFHS* having different *Hcp/d* ratios and their comparison with that of *CPFHS*. The figure clearly shows that the thermal resistance decreases with increasing *Re* and *Hcp/d* ratio. This is for the reason that the rising *Re* and *Hcp/d* ratio means increasing turbulence intensity and heat transfer area. The results indicate that R_{th} is decreased by 192.30%, 162.17%, 135.95%, 105.99% and 83.52% for *Hcp/d*=0.167, 0.333, 0.500, 0.667 and 0.833 compared to the cylindrical pin fins at *Re* = 8000, respectively.

4.6. Hydro thermal performance evaluation

Such as a thermal system, the heat sinks need a judge parameter between the augmentations of Nusselt number as the heat transfer coefficient and pressure drop. The hydrothermal performance factor (η) presents a good parameter, which is largely used to select the optimum configuration. Fig. 9 depicts the variation of the hydrothermal performance factor (η) versus Reynolds number (*Re*) for various *Hcp/d*. As shown in the figure, η is greater than the unit for all of the proposed configurations, since these configurations are better than the cylindrical pin fins. The results indicate that η increases with decreasing *Hcp/d* ratio. The case of *Hcp/d*=0.167, at *Re*=8000 ensures highest value of hydro thermal performance factor (η) by 1.51 which is merits to use in heat sinks designing in the future.

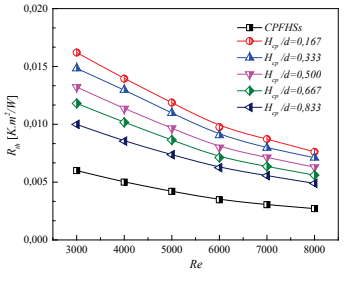

Figure 8: Thermal resistance (R_{th}) vs. Reynolds number (*Re*).

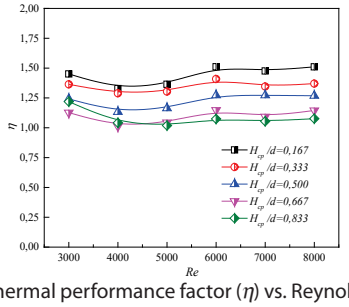

Figure 9: Thermal performance factor (η) vs. Reynolds number (*Re*).

5. Conclusion

The hydrothermal characteristics of heat sinks with various shaped fins were determined numerically. The conical and cylindrical shapes of fins were considered and explored. The performances of five geometrical configurations of conical fins with varying conical ratio (*Hcp/d* = 0.167, 0.333, 0.500, 0.667 and 0.833) were compared against those of the cylindrical fins. A special attention was paid to the distribution and amounts of Nusselt number, thermal fields, thermal resistance, pressure losses, and the hydrothermal performance factor. The main results are resumed as follows:

- *The conical fins resulted less pressure losses than the cylindrical fins. However, the rise of (Hcp/d) ratio induced an increase in the pressure drop. At the highest value of Reynolds number considered here (Re = 8000), the amounts of pressure drop for the conical fins were reduced by 343.32% and 100.38% for Hcp/d = 0.167 and 0.833, respectively (against the cylindrical fins).*
- *The increasing Re and Hcp/d ratio yielded a decrease in the thermal resistance. At Re = 8000 and compared to the cylindrical fins, the values of the thermal resistance were decreased by 192.30% to 83.52% for Hcp/d = 0.167 and 0.833, respectively.*
- *The values of the hydrothermal performance factor (η) for the conical fins are greater than those of the cylindrical fins.*
- *The decreasing Hcp/d ratio yielded an increase in (η) values, where the highest value of the hydrothermal performance factor η = 1.51 was obtained with the case Hcp/d = 0.167 at Re = 8,000.*
- *Finally, these promising results allow us selecting and recommending the case with Hcp/d = 0.167 in designing the future heat sinks.*

Nomenclature

χ	Cartesian coordinate vector [m]
υ	Kinematic viscosity [m2/s]
p	Modified kinematic pressure [m2/s2]
Δp	Pressure drop [Pa]
ω	Specific dissipation rate [1/s]
α	Thermal diffusivity [m2/s]
k	Turbulent kinetic energy [m2/s2]
q''	Heat flux [W/m2]
μ	Dynamic viscosity [kg/(m·s)]
A	Cross flow section [m2]
Ac	Heat transfer surface [m2]
C_p	Specific heat [J/(kg·K)]
D	Diameter of cylindrical pin fins [m]
D_h	Hydraulic diameter [m]
H	Height of channel inlet [m]
Nu	Nusselt number

Re	Reynolds number
R_{th}	Thermal resistance [K.m2/W]
T	Temperature [K]
U	Mean velocity [m/s]
λ	Thermal conductivity [W/(m·K)]
ρ	Density [kg/m3]

Subscript

i, j	Tensor index
in	Inlet
out	Outlet
s	Solid
w	Wall

Abbreviations

CFD	Computational Fluid Dynamics
CPF	Cylindrical pin fin
CPFHS	Cylindrical pin fin heat sink
Co-PFHS	Conical pin fin heat sink
LHTAs	Lower hear transfer areas
PFHS	Pin fin heat sink

References

[1] Ho, C. J., Hsu, S. T., Jang, J. H., Hosseini, S. F., Yan, W. M., (2020). Experimental study on thermal performance of water-based nano-PCM emulsion flow in multichannel heat sinks with parallel and divergent rectangular mini-channels, International Journal of Heat and Mass Transfer, 146, 118861.

[2] Kuznetsov, V. V., Shamirzaev, A. S., (2010). Flow boiling heat transfer of refrigerant R21 in microchannel heat sink, Journal of Engineering Thermophysics, 19, 306–317.

[3] Bellahcene, L., Sahel, D., Yousfi, A., (2021). Numerical Study of Shell and Tube Heat Exchanger Performance Enhancement Using Nanofluids and Baffling Technique, Journal of Advanced Research in Fluid Mechanics and Thermal Sciences, 80, 42–55.

[4] Wang, S., Xing, Y., Hao, Z., Yin, J., Hou, X., Wang, Z., (2021). Experimental study on the thermal performance of PCMs based heat sink using higher alcohol/graphite foam, Applied Thermal Engineering, 198, 117452.

[5] Fadhil, A. M., Khalil, W. H., Al-damook, A., (2019). The hydraulic-thermal performance of miniature compact heat sinks using SiO2-water nanofluids, Heat Transfer - Asian Research, 48, 3101–3114.

[6] Babar, H., Ali, H. M., (2019). Airfoil shaped pin-fin heat sink: Potential evaluation of ferric oxide and titania nanofluids, Energy Conversion and Management, 202, 112194.

[7] Jung, S. Y., Park, H., (2021). Experimental investigation of heat transfer of Al2O3 nanofluid in a microchannel heat sink, International Journal of Heat and Mass Transfer, 179, 121729.

[8] Murali, K. V., Sandeep K. M., Muthalagu, R., Senthil K. P., Mounika, R., (2021). Numerical study of fluid flow and heat transfer for flow of Cu-Al2O3-water hybrid nanofluid in a microchannel heat sink, Materials Today, (In Press), 1–5.

[9] Bahiraei, M., Jamshidmofid, M., Dahari, M., (2020). Second law analysis of hybrid nanofluid flow in a microchannel heat sink integrated with ribs and secondary channels for utilization in miniature thermal devices, Chemical Engineering and Processing - Process Intensification, 153, 107963.

[10] Kumar, V., Sarkar, J., Yan, W. M., (2021). Thermal-hydraulic behavior of lotus like structured rGO-ZnO composite dispersed hybrid nanofluid in mini channel heat sink, International Journal of Thermal Sciences, 164, 106886.

[11] Ozguc, S., Pan, L., Weibel, J. A., (2021). Optimization of permeable membrane microchannel heat sinks for additive manufacturing, Applied Thermal Engineering, 198, 117490.

[12] Qiu, T., Wen, D., Hong, W., Liu, Y., (2020). Heat transfer performance of a porous copper micro-channel heat sink, Journal of Thermal Analysis and Calorimetry, 139, 1453–1462.

[13] Khattak, Z., Ali, H. M., (2019). Air cooled heat sink geometries subjected to forced flow: A critical review, International Journal of Heat and Mass Transfer, 130, 141–161.

[14] Alihosseini, Y., Zabetian Targhi, M., Heyhat, M. M., Ghorbani, N., (2020). Effect of a micro heat sink geometric design on thermo-hydraulic performance: A review, Applied Thermal Engineering, 170, 114974.

[15] Sahel, D., Bellahcene, L., Yousfi, A., Subasi, A., (2021). Numerical investigation and optimization of a heat sink having hemispherical pin fins, International Communications in Heat and Mass Transfer , 122, 105133.

[16] Huang, C. H., Huang, Y. R., (2021). An optimum design problem in estimating the shape of perforated pins and splitters in a plate-pin-fin heat sink, International Journal of Thermal Sciences, 170, 107096.

[17] Al-Damook, A., Summers1, J.L., Kapur, N., Thomson, H., (2016). Effect of different perforations shapes on the thermal-hydraulic performance of perforated pinned heat sinks, Journal of Multidisciplinary Engineering Science and Technology, 3, 4466–4474.

[18] Maji, A., Bhanja, D., Patowari, P. K., (2019). Effect of knurled fin surface on thermal performance of perforated fin heat sink, Journal of Thermophysics and Heat Transfer, 33, 580–598.

[19] Chin, S. B., Foo, J. J., Lai, Y. L., Yong, T. K. K., (2013). Forced convective heat transfer enhancement with perforated pin fins, Heat and Mass Transfer, 49, 1447–1458.

[20] Kore, S. S., Yadav, R., Chinchanikar, S., Tipole, P., Dhole, V., (2020). Experimental investigations of conical perforations on the thermal performance of cylindrical pin fin heat sink,"

International Journal of Ambient Energy (Article in press).

[21] Shaeri, M. R., Bonner, R., (2017). Heat transfer and pressure drop in laterally perforated-finned heat sinks across different flow regimes," International Communications in Heat and Mass Transfer, 87, 220–227.

[22] Al-Damook, A., Summers, J. L., Kapur, N., Thompson, H., (2016). Effect of temperature-dependent air properties on the accuracy of numerical simulations of thermal airflows over pinned heat sinks, International Communications in Heat and Mass Transfer, 78, 163–167.

[23] Sahel, D., (2021). Thermal Performance Assessment of a Tubular Heat Exchanger Fitted with Flower Baffles, Journal of Thermophysics and Heat Transfer, 35 ,726–734.

[24] Sahel, D., Ameur, H., Alem, K., (2021). Enhancement of the hydrothermal characteristics of fin-and-tube heat exchangers by vortex generators, Journal of Thermophysics and Heat Transfer, 35, 152–163.

[25] Alem, K., Sahel, D., Nemdili, A., Ameur, H., (2018). CFD investigations of thermal and dynamic behaviors in a tubular heat exchanger with butterfly baffles, Frontiers in Heat and Mass Transfer, 10 , 1-7.

[26] Ameur, H., Sahel, D., Menni, Y., (2021). Numerical Investigation of the performance of perforated baffles in a plate-fin heat exchanger, Thermal Science, 25 (Part B), 3629–3641.

[27] Sahel, D., Ameur, H., Touhami, B., (2018). Effect of the size of graded baffles on the performance of channel heat exchangers, Thermal Science, 2, 767–775.

[28] Ameur, H., Sahel, D., Menni, Y., (2020). Enhancement of the cooling of shear-thinning fluids in channel heat exchangers by using the V-baffling technique, Thermal Science and Engineering Progress, 18, 100534.

[29] Karami, M., Tashakor, S., Afsari, A., Hashemi-Tilehnoee, M., (2019). Effect of the baffle on the performance of a micro pin fin heat sink, Thermal Science and Engineering Progress,14, 100417.

[30] Khoshvaght-Aliabadi, M., Ahmadian, E., Sartipzadeh, O., (2017). Effects of different pin-fin interruptions on performance of a nanofluid-cooled zigzag miniature heat sink (MHS), International Communications in Heat and Mass Transfer, 81, 19–27.

[31] Khan, A. A., Kim, S. M., Kim, K. Y., (2016). Performance analysis of a microchannel heat sink with various rib configurations, Journal of Thermophysics and Heat Transfer, 30, 782–790.

[32] Subasi, A., Ozsipahi, M., Sahin, B., Gunes, H., (2017). Performance evaluation of RANS-based turbulence models in simulating a honeycomb heat sink, Heat and Mass Transfer, 53, 2435–2443. https://doi.org/10.1007/s00231-017-1969-8

[33] Saravanan, V., Umesh, C. K., (2018). Numerical comparison for thermo-hydraulic performance of pin fin heat sink with micro channel pin fin heat sink, Proceedings in Engineering Sciences, 43, 1–15.

[34] Yousfi, A., Sahel, D., Mellal, M., (2019). Effects of a pyramidal pin fins on CPU heat sink performances, Journal of Advanced Research in Fluid Mechanics and Thermal Sciences, 63, 260–273.

[35] Leong, K. Y., Chew, S. P., Gurunathan, B. A., Ku Ahmad, K. Z., Ong, H. C., (2019). An experimental approach to investigate thermal performance of paraffin wax and 1-hexadecanol based heat sinks for cooling of electronic system, International Communications in Heat and Mass Transfer, 109, 104365.

[36] Shi, X., Li, S., Mu, Y., Yin, B., (2019). Geometry parameters optimization for a microchannel heat sink with secondary flow channel, International Communications in Heat and Mass Transfer, 104, 2019, 89–100.

[37] Sathe, A., Sanap, S., (2020). Experimental analysis of effect of slitted rectangular fins on heat sink under natural convection heat transfer, International Journal of Ambient Energy (Article in press).

[38] Vinoth, R., Senthil Kumar, D., (2017). Channel cross section effect on heat transfer performance of oblique finned microchannel heat sink, International Communications in Heat and Mass Transfer, 87, 270–276.

[39] Ozsipahi, M., Subasi, A., Gunes, H., Sahin, B., (2018). Numerical investigation of hydraulic and thermal performance of a honeycomb heat sink, International Journal of Thermal Sciences, 134, 500–506.

[40] Derakhshanpour, K., Kamali, R., Eslami, M., (2020). Effect of rib shape and fillet radius on thermal-hydrodynamic performance of microchannel heat sinks: A CFD study, International Communications in Heat and Mass Transfer. 119, 104928.

[41] CFD Module User's guide. Comsol Multiphysics v.5.4. Comsol AB, Stockholm, Sweden.